

Electronic Supplementary Information

Band Engineering of Perovskite-type Transition Metal Oxynitrides for Photocatalytic Overall Water Splitting

Chengsi Pan,^a Tsuyoshi Takata,^{*a} Kazunori Kumamoto,^b Su Su Khine Ma,^{b,c}
Koichiro Ueda,^{b,c} Tsutomu Minegishi,^b Mamiko Nakabayashi,^{b,d} Takao
Matsumoto,^d Naoya Shibata,^d Yuichi Ikuhara^d and Kazunari Domen^{*a,b,c}

^a Global Research Center for Environment and Energy based on Nanomaterials Science (GREEN), National Institute for Materials Science (NIMS), 1-1 Namiki, Tsukuba-city, Ibaraki 305-0044, Japan

^b Department of Chemical System Engineering, School of Engineering, The University of Tokyo, 7-3-1 Hongo, Bunkyo-ku 113-8656, Japan

^c Japan Technological Research Association of Artificial Photosynthetic Chemical Process (ARPCHEM), 5-1-5 Kashiwanoha, Kashiwa-city, Ciba 227-8589, Japan

^d Institute of Engineering Innovation, School of Engineering, The University of Tokyo, 2-11-16, Yayoi, Bunkyo-ku, 113-8656, Japan

Experimental Methods

S1 Sample preparation for STEM analysis

For Cs-corrected FE-STEM, a thinly sliced sample was used to ensure sufficient transmittance of the electron beam. The sample powder was mixed with a G2 epoxy resin, which was subsequently plasticized by drying at 353 K for 10 min and subsequent heating at 423 K for 1 h. Then, the embedded sample was thinly sliced by accelerated Ar ions using an ion slicer (EM-09100IS, JEOL Ltd.). For EDX analysis, the sample particles were spread on a carbon film supported by a molybdenum mesh.

S2 ABF-STEM image simulation

ABF-STEM image simulation was carried out with the QSTEM software package developed by Koch.^{s1} The structures used for simulation are shown in the Fig. 1b inset. The values we used in QSTEM were: acceleration voltage, 200 kV; ABF collection angle, 0-40 mrad; defocus, -60 nm; Cs, 1 mm; Cc, 1.0 mm; convergence angle, 15 mrad; and 400 × 400 samples across a 50 × 50 Å sample size. The slice thickness was set at 1.927 Å. The QSTEM package offered the option of simulating a thermal diffuse scattering temperature of 300 K.

S3 Theoretical calculation

The DFT calculation was performed on CASTEP. The crystal parameters (such as the lattice constants, the space group, the positions for La, Mg/Ta and O/N atoms) used for the calculations are obtained from ref. s2 and s3. A 3 × 2 × 1 supercell with 120 atoms was built to perform optimization. According to the literature^{s3}, two types of B-sites are adjacently arranged in the LaMg_{1/3}Ta_{2/3}O₂N structure. The occupancy of Mg²⁺/Ta⁵⁺ at each B-site is refined to be 0.356: 0.644 and 0.310: 0.690, respectively. In our supercell, in order to simplify calculations, Mg²⁺ and Ta⁵⁺ ions are symmetrically distributed over all B-sites, leading to occupancy of Mg²⁺/Ta⁵⁺ at each type of B-sites to be 1:2. The O²⁻ and N³⁻ ions are then manually added to all anionic sites to form a reported stable configuration^{s4}. Namely, Mg²⁺ ions are surrounded by six O²⁻ ions, while the leftover O²⁻ ions and all the N³⁻ ions are symmetrically distributed between Ta⁵⁺ ions. The Perdew-Burke-Ernzerh of generalized gradient approximation (PBE-GGA) was used to describe the exchange and correlation energy of the electrons. A 1 × 2 × 2 k-point sampling of the Brillouin zone was used. The calculations were done with designed nonlocal norm-conserving pseudopotentials. The cutoff energy was 380 eV.

Reference

s1 C. Koch, *Ph.D. Thesis*, Arizona State University, 2002.

s2 Y. Kim and P. Woodward, *J. Solid State Chem.*, 2007, **180**, 3224.

s3 Y. Kim, *Ph.D. Thesis*, The Ohio State University, 2005.

s4 H. Wolff, M. Lerch, H. Schilling, C. Bähz and R. Dronskowski, *J. Solid State Chem.*, 2008, **181**, 2684.

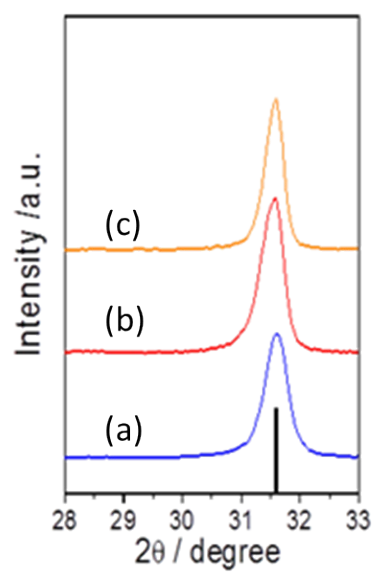


Figure S1 Enlarged XRD patterns of Figure 1b. $\text{LaMg}_{0.33}\text{Ta}_{0.67}\text{O}_2\text{N}$ samples nitrided from oxide

precursors that was calcined at different temperatures (a) 973K, (b) 1073K, (c) 1173K.

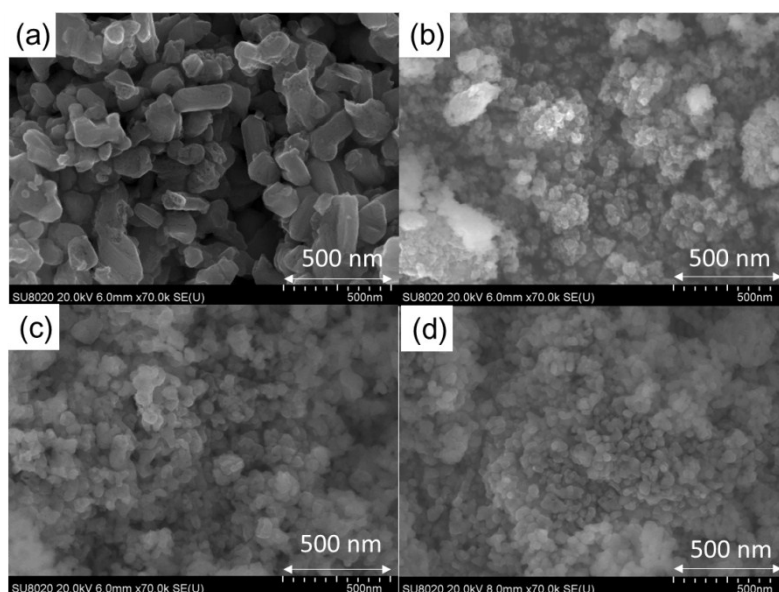


Figure S2 SEM images of $\text{LaMg}_x\text{Ta}_{1-x}\text{O}_{1+3x}\text{N}_{2-3x}$ (a) $x=0$, (b) $x=0.1$, (c) $x=0.33$, (d) $x=0.5$.

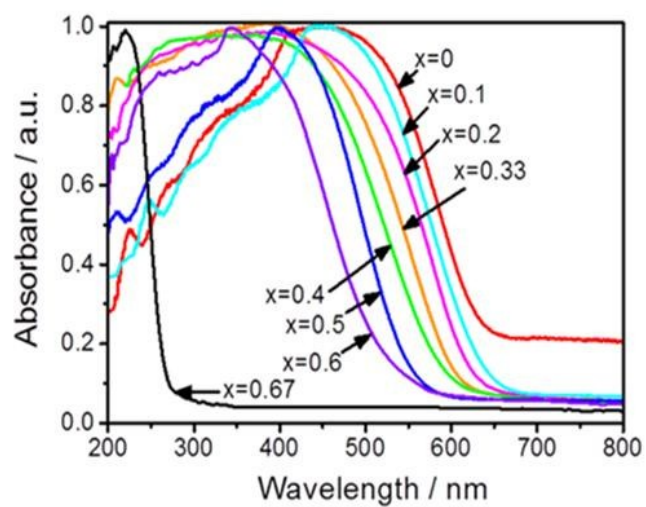


Figure S3 UV-visible diffuse reflectance spectra of $\text{LaMg}_x\text{Ta}_{1-x}\text{O}_{1+3x}\text{N}_{2-3x}$ series.

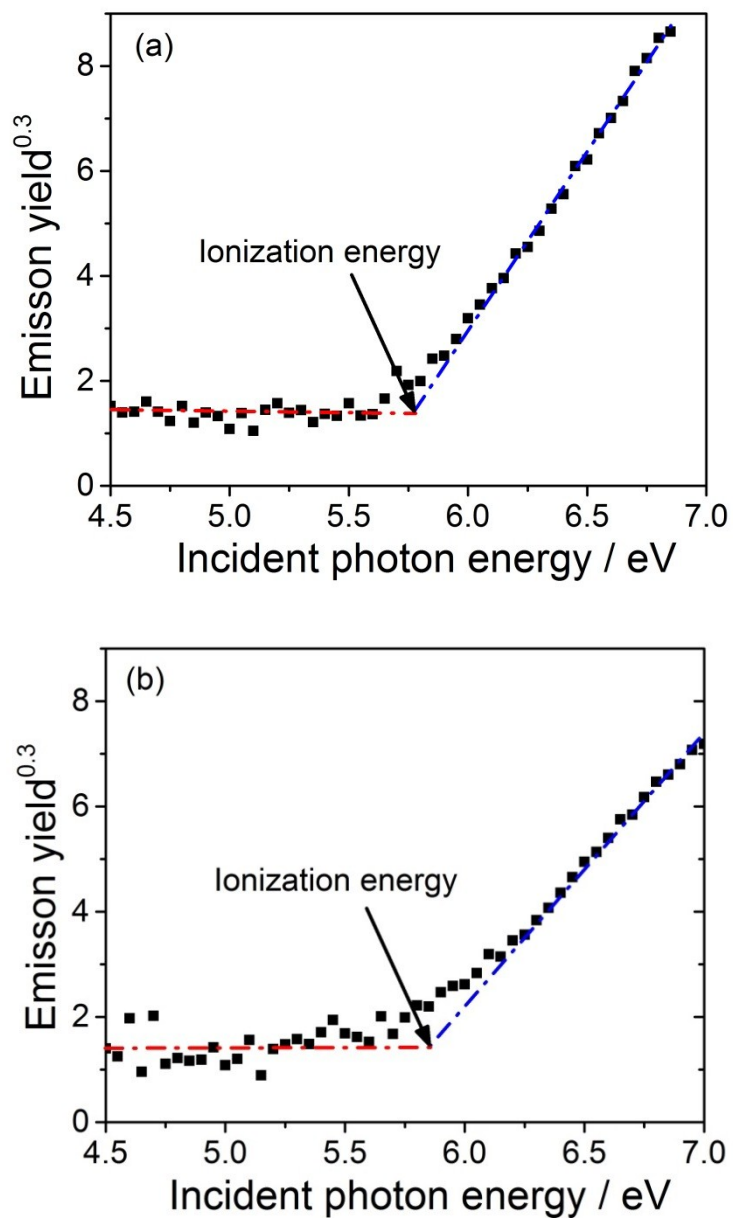


Figure S4 PESA spectra of LaTaON_2 (a) and $\text{LaMg}_{0.33}\text{Ta}_{0.67}\text{O}_2\text{N}$ (b) electrodes fabricated by particle transfer method. The ionization potential which equal to VBM potential can be converted to the potential against a normal hydrogen electrode (NHE) by $E / \text{V vs. NHE} = E / \text{V vs. vacuum level} - 4.44 / \text{V}$.

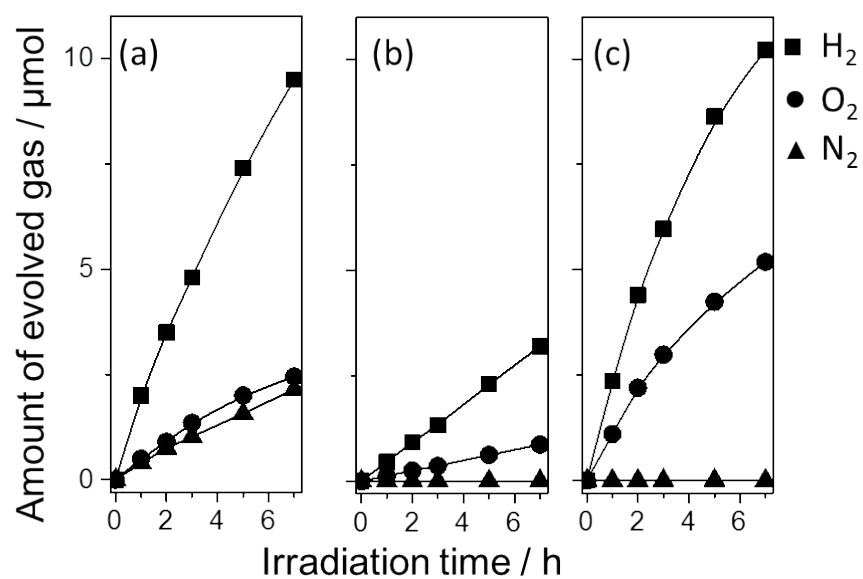


Figure S5 Time courses of water splitting on (a) $\text{CoO}_2/\text{RhCrO}_y/\text{LaMg}_{0.33}\text{Ta}_{0.67}\text{O}_2\text{N}$, (b) $\text{TiO}_2/\text{CoO}_2/\text{RhCrO}_y/\text{LaMg}_{0.33}\text{Ta}_{0.67}\text{O}_2\text{N}$ and (c) $\text{TiO}_2/\text{RhCrO}_y/\text{LaMg}_{0.33}\text{Ta}_{0.67}\text{O}_2\text{N}$. Reaction conditions: catalyst, 0.2 g; reaction solution, pure water (250 mL); light source, Xe lamp (300 W, $\lambda \geq 300$ nm); side irradiation-type reaction vessel made of Pyrex.

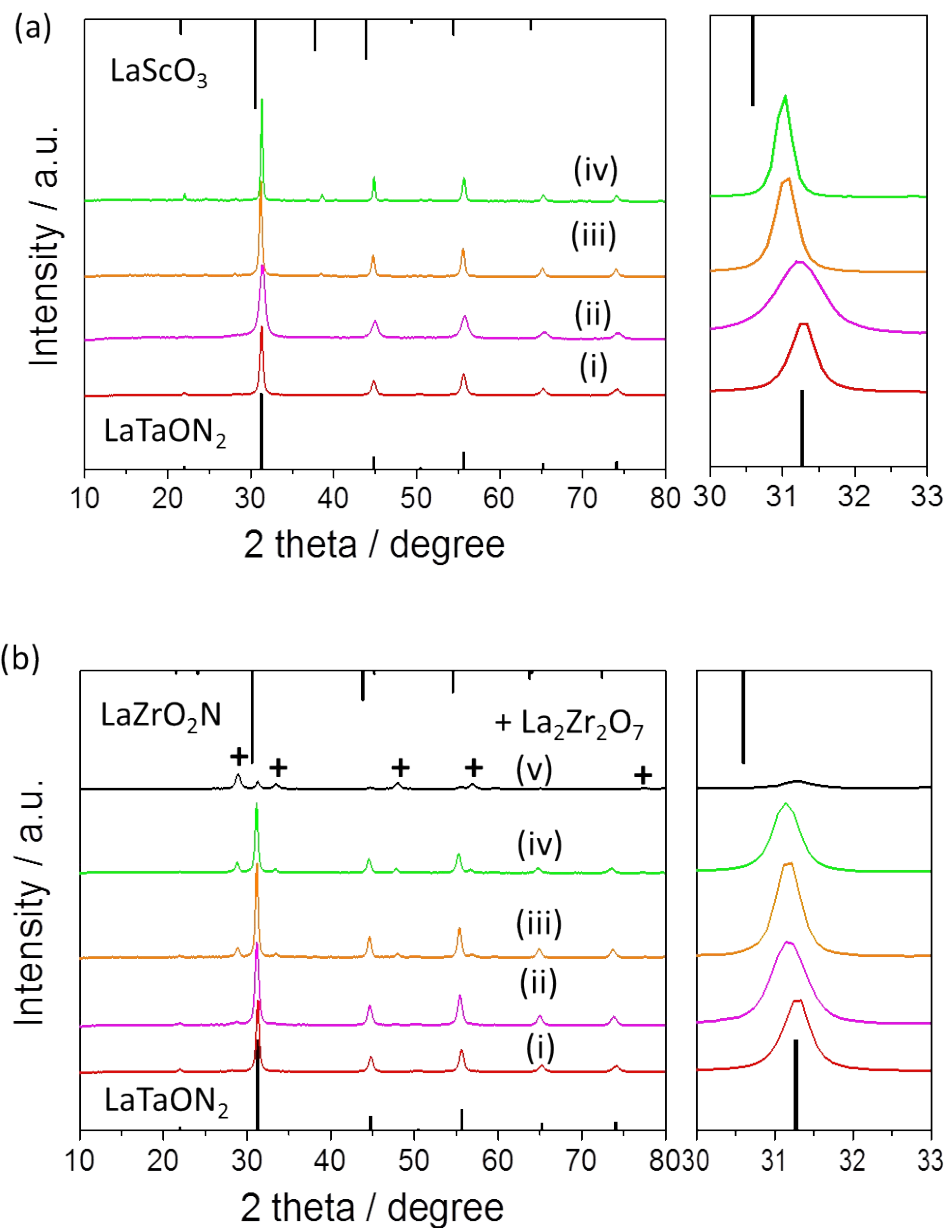


Figure S6 XRD of (a) $\text{LaSc}_x\text{Ta}_{1-x}\text{O}_{1+2x}\text{N}_{2-2x}$ with different Sc content (x), (i) 0.25, (ii) 0.33 (iii) 0.5, (iv) 0.75; and (b) $\text{LaZr}_x\text{Ta}_{1-x}\text{O}_{1+x}\text{N}_{2-x}$ with different Zr content (x), (i) 0.05, (ii) 0.25 (iii) 0.33, (iv) 0.50, (v) 0.75.

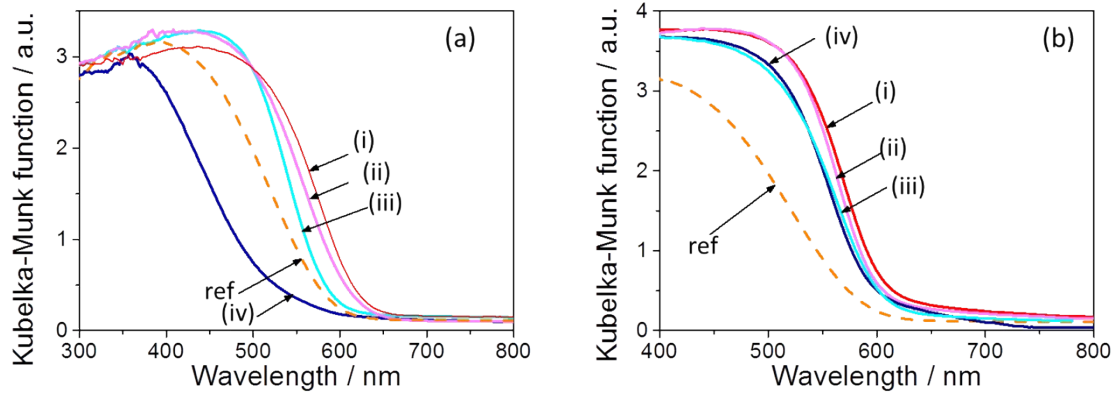


Figure S7 UV-Vis DRS of (a) $\text{LaSc}_x\text{Ta}_{1-x}\text{O}_{1+2x}\text{N}_{2-2x}$ with different Sc content(x), (i) 0.25, (ii) 0.33 (iii) 0.5, (iv) 0.75; and (b) $\text{LaZr}_x\text{Ta}_{1-x}\text{O}_{1+x}\text{N}_{2-x}$ with different Zr content(x), (i) 0.05, (ii) 0.25 (iii) 0.33, (iv) 0.50. Ref. is the absorption spectrum of $\text{LaMg}_{0.33}\text{Ta}_{0.67}\text{O}_2\text{N}$.

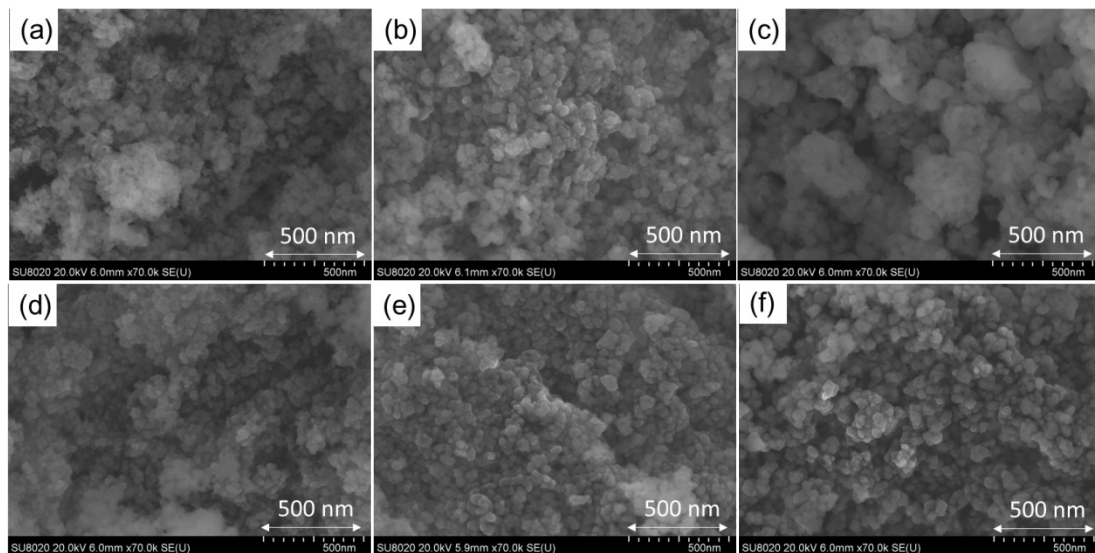


Figure S8 SEM images of $\text{LaSc}_x\text{Ta}_{1-x}\text{O}_{1+2x}\text{N}_{2-2x}$ (a-c): (a) $x=0.33$, (b) $x=0.5$, (c) $x=0.75$; and $\text{LaZr}_x\text{Ta}_{1-x}\text{O}_{1+x}\text{N}_{2-x}$ (d-f): (d) $x=0.25$, (e) $x=0.33$, (f) $x=0.5$.

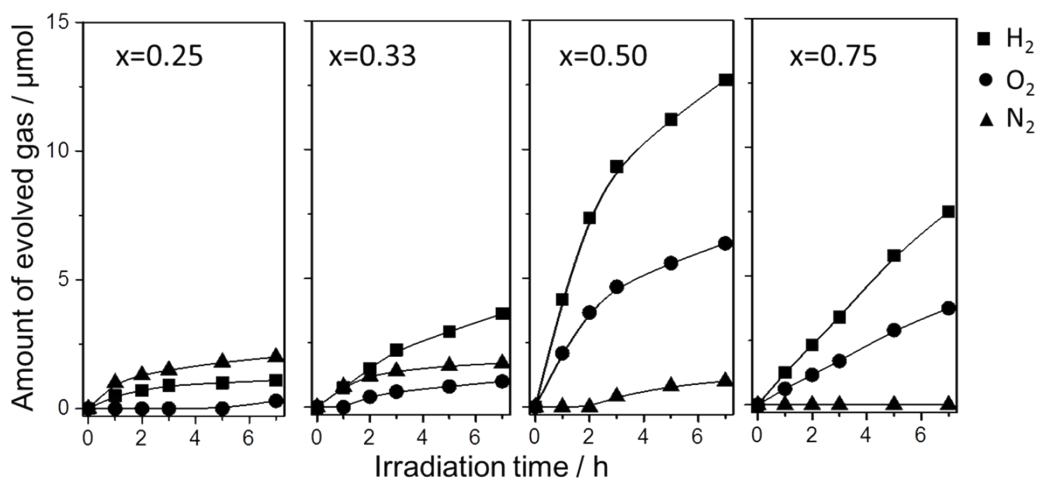


Figure S9 Time courses of water splitting on $\text{TiO}_2/\text{RhCrO}_y/\text{LaSc}_x\text{Ta}_{1-x}\text{O}_{1+2x}\text{N}_{2-2x}$. Reaction conditions: catalyst, 0.2 g; reaction solution, pure water (250 mL); light source, Xe lamp (300 W, $\lambda \geq 300$ nm); side irradiation-type reaction vessel made of Pyrex.

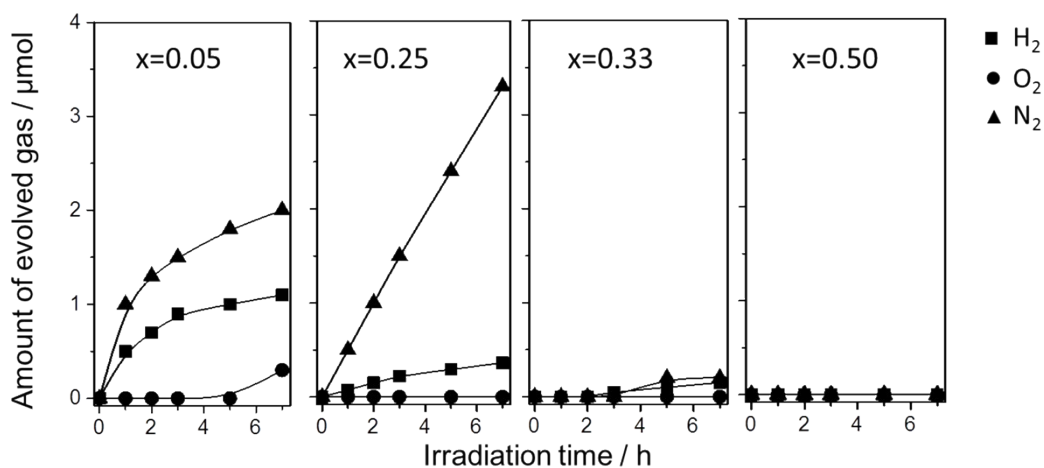


Figure S10 Time courses of water splitting on $\text{TiO}_2/\text{RhCrO}_y/\text{LaZr}_x\text{Ta}_{1-x}\text{O}_{1+x}\text{N}_{2-x}$. Reaction conditions: catalyst, 0.2 g; reaction solution, pure water (250 mL); light source, Xe lamp (300 W, $\lambda \geq 300$ nm); side irradiation-type reaction vessel made of Pyrex.